PHOTOGRAMMETRIC RECONSTRUCTION AND MULTI-TEMPORAL COMPARISON OF BRENVA GLACIER (ITALY) FROM ARCHIVE PHOTOS

A. Malekian [1], D. Fugazza [2], M. Scaioni [3]

[1] Politecnico di Milano, Lecco Campus, via G. Previati 1/c, 23900 Lecco, Italy - arsalan.malekian@mail.polimi.it
[2] Università degli Studi di Milano, Department of Environmental Science and Policy, Via Celoria 2, Milano, Italy - davide.fugazza@unimi.it
[3] Politecnico di Milano, Dept. of Architecture, Built Environment and Construction Engineering, via Ponzio 31, 20133 Milano, Italy - marco.scaioni@polimi.it

Commission IV, WG IV/3

KEY WORDS: Aerial Images, 3D Reconstruction, Photogrammetry, Glacier Monitoring, Archive Photos, Structure-from-Motion.

ABSTRACT:

Since climate change has a significant impact on glaciers, it is essential to track their morphological change by identifying variations in ice mass. In combination with modern photogrammetric approaches, such as Structure-from-Motion (SfM) and Multi-View-Stereo (MVS) dense matching, historical aerial photographs may offer useful information for this objective. Point clouds of the 3D surface of the glaciers may be used to track changes in thickness and height during years. By using appropriate methods for calculating the distances between pairs of point clouds, this operation may be completed. Here, an Alpine glacier massif on Mount Blanc in the Italian Alps was chosen as the case study. National Geographic and the Forestry Institute of France (IGNF) provided seven data sets of digitized analog aerial photos. These were chosen, downloaded, and utilized for photogrammetric analysis. These data sets span almost 40 years, from 1967 to 2006, in total. While the change in ice thickness of these glaciers was relatively small until the mid-1990s, this study revealed an increasing reduction rate at the beginning of 21st century. This paper describes the adopted methodological approach for photogrammetric reconstruction, quality assessment and point cloud comparison. One of the two major glaciers in the considered group (Brenva Glacier) has been focused in this paper as case study.

1. INTRODUCTION

In the last decade the cryosphere has undergone dramatic retreat as consequence of global climate change. The Himalayan and other Alpine glaciers, as well as the Antarctic and Artic regions, were all impacted by this mechanism.

When it comes to glaciers in the European Alps, their retreat has a significant effect on the local natural and human environment. Changes of local ecosystems, reduction of water resources, impact on regional economy and tourism, natural hazards related to weakening of the ice bodies are only some out the major and more evident results of this dramatic change. On 3rd July 2022 the sudden collapse of Marmolada Glacier killed 11 hikers in the Dolomites (Italy), but it might have resulted in even more severe consequence due to the presence of a water basin below (Wikipedia, 2022). This dramatic event, among previous ones, brought to the attention of the entire community how this process has also a direct impact on the human and social life, besides the impact on the environment.

While active mitigation actions at local level may give only a limited contribution to invert this disruption process, the analysis, assessment and monitoring of the conditions of Alpine glaciers may help understand the dynamics and the relationships with causative factors. This knowledge is really valuable to better detect hazards and critical areas, as already demonstrated in previous studies (e.g., see Scaioni et al., 2019).

Today, a variety of sensor types may be placed on glacial and periglacial regions to collect physical data that is valuable for modeling the hydraulic behavior of an Alpine glacier and understanding its environmental conditions. In addition, proximal and remote sensing methods enable the collection of data for the extension of the ice cover and the 3D reconstruction of the topographic surface. The comparison of these items of information collected within time offer the opportunity to detect volumetric and superficial changes (Fugazza et al., 2018).

For creating 3D models of glaciers, the two major methods are photogrammetry and laser scanning (LS). Both may work based on data recorded by platforms to be operated on the ground (*terrestrial* photogrammetry and LS), from *drones*, and manned aircrafts (*aerial* photogrammetry and LS). The photogrammetric reconstruction can be also applied with *high* (and *very-high*) *resolution satellite imagery*. *Satellite laser altimetry* (e.g., ICESAT 1/2, JAXA/NTT DATA missions) may provide more sparse observations useful for studying large glaciers and the Artic/Antarctic regions, but they are less useful for investigating smaller Alpine glaciers. Both photogrammetry and LS may provide *dense point clouds* describing the outer topographic surface of a glacier and its surrounding areas (digital surface model – DSM).

Itis beyond the aim of this paper to analyse and compare these techniques. The reader is suggested to look in the wide bibliography about these topics (Fugazza et al., 2018). The concept that it is highlighted here refers to the fact the planning data acquisition to record new geometric data about Alpine glaciers may rely on the photogrammetry and LS. But in the case a *retrospective study* should be conducted, historical data need to be found. These may consist in different *data sources* or already processed *products*. In the first group the following types of data could be available:

1. *Aerial photos* from archives of mapping agencies, public administrations and private companies; these may be in digital or analogue format, the latter to be digitized by using photogrammetric scanners if necessary; and
2. *High/very-high resolution satellite imagery* from image providers.

Among *products* the following may be looked for:

1. *Digital elevation models* (DEM) of the glacier region, obtained from Geomatics techniques and interpolated along a regular grid;
2. *DSM* or other *sparce point coordinates* obtained in previous scientific studies and made available by owners; and
3. Topographic maps of the glacier region, whether digital or analog, that include contour lines for 3D modelling; Generally, the quality of these maps' quality may be fairly inadequate for glaciological applications, especially if they date back to the early half of the XX century. On the other hand, prior to the 1950s, topographic maps were sometimes the only information accessible.

When a retrospective study should be afforded, scientists should look for the availability of these existing data sets. This paper would like to focus on one specific data source, i.e., *archive aerial photos* (see Subsect. 1.1). An application to study the major Alpine glacier (Brenva Glacier) in the Italian Alps near the French border is shown. These results belong to a wider investigation covering other glaciers in the same areas, which are focused on other publication (Malekian et al., 2022). Due to the region's proximity to France, a sizable online database of historical photographs administered by the National Geographic and Forestry Institute of France (IGNF) is accessible.

1.1 Archive Aerial Photos for Glaciological Studies

One of the earliest data sources for glacier monitoring is archive aerial photographs. They are undoubtedly very helpful for observing glaciers in terms of extension, length, volume, and mass change (Fey et al., 2017). Typically, these archives are made up of old aerial photos used for regional photogrammetric topographic mapping efforts. Utilizing cutting-edge digital photogrammetric techniques like Structure-from-Motion (SfM) and Multi-View Stereo (MVS) dense matching, they may be utilized in glaciological investigations to produce geometrically accurate 3D models of glaciers (Eltner et al., 2015).

The oldest photos in the collection were taken using analogue film cameras. Up to the first decade of the twenty-first century, they were considered the cutting edge of mapping technology. However, since the 1990s, digital photogrammetric workstations have increasingly replaced analytical stereo plotters as the industry standard for both image orientation and stereoplotting (Kraus, 2008). Photogrammetric scanners converted analog photograms into digital photos. In the last two decades, digital airborne cameras (DACs), which immediately record digital aerial images, have begun to replace analog cameras.

Comprehensive volume and elevation studies have already been computed using old aerial photographs. Since the 1950s, aerial photographs have been used to analyze sixteen Antarctic glaciers (Fox et al., 2008). Based on continuous photogrammetric processing of aerial photographs, DEMs and orthophotos for a glacier in Sweden were produced between 1959 and 1990. (Koblet et al., 2010). Additionally, for the purpose of 3D modeling of glaciers and change analysis, a dataset consisting of scans of 300 (analog) aerial photographs taken over the province of Trento between August and October 1954 by the U.S. Air Force was employed (Poli et al., 2020).

This study explores the possibility of creating 3D models of Alpine glaciers from historical aerial photographs. These models may then be compared between historical periods to identify morphological and volumetric changes.

2. CASE STUDY

2.1 Brenva Glacier

The primary objective of this investigation is to assess the geometric variations of the Brenva Glaciers in the Val Veny region (Figure 1), a lateral valley of the Mont Blanc massif in the Aosta Valley (Italy). Malekian et al. provide much material on this topic (2022). A valley glacier on the Alps' southern edge is called the Brenva Glacier. It is the second-longest and eighth-largest glacier in Italy and flows into Val Veny in Entrèves, close to the town of Courmayeur. Throughout the millennia, it has experienced a number of big rock avalanches that have shaped the glacier and changed its flow. The Brenva glacier is a 7.5 km long valley glacier with a tongue width of 0.5 km on average and a maximum width of 2.15 km. The tongue is divided transversely into two areas by a rock step called the "Pierre a Moulin" between 2,460 and 2,550 meters above sea level (Figure. 2). The down-valley sector lacks dynamic continuity since it is cut off from the main body, and the lowest half has been totally covered by debris. (Giani et al., 2001).

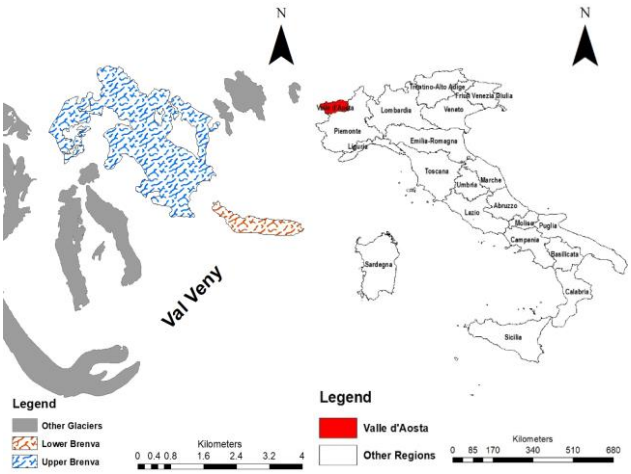

Figure 1. The location of the Brenva glacier, between other glaciers in the area, in the Aosta Valley in Italy.

Figure 2. The separation of Brenva Glacier in the middle part by a rock step called 'Pierre a Moulin.'

It is important to remember that Brenva Glacier has endured numerous devastating events throughout its history. On the afternoon of November 14, 1920, a large rockfall flowed up the

opposite valley side from the Brenva Glacier after detaching from the Mont Blanc's east face near Grand Pillier d'Angle, close to the 1997 scar (Evans and Clague, 1998). A significant rock-ice avalanche hit the Brenva Glacier twice in the 20th century, the most recent incident being in 2009. The Mont Blanc East Face at 3,725 meters above sea level saw thawing permafrost (0 to -5 degrees Celsius) on January 18, 1997, resulting in a large Alpine avalanche occurrence in the upper Aosta Valley. The collective action generated an enormous amount of snow and ice, creating a powder avalanche that had a total volume of 6 to 7 million m3 (Barla, 2000). 5.500 meters and 2.150 meters, respectively, were moved horizontally and vertically, with a 21.6 degree reach angle. A portion of the rock-ice avalanche flooded the right lateral moraine.

2.2 Datasets for Photogrammetry

The historical aerial photographs of the Val Veny included in this study came from a variety of airborne flights conducted between 1967 and 2006. Digital images are made available via the IGNF's WEB site. Every dataset comes with a calibration certificate that lists the camera and lens that were used (Kraus, 2008). While mission information is typically restricted to the average flight height, photo scale, and side overlap, image orientation parameters computed after aerial triangulation or recorded by onboard GNSS/INS (Global Navigation Satellite System/Inertial Navigation System) sensors are not typically provided. The majority of missions were carried out using analog film cameras of various kinds, all of which had a standard focal length (about 150 mm) and film format (23 cm x 23 cm). Photogrammetric scanners were then used to convert analog panchromatic or color photos into digital photos. The chosen pixel size was in the range of 20 m. Using a frame DAC, data sets gathered over the previous 20 years—like the one from 2006—were directly recorded. All adopted photogrammetric data sets are shown in Table 1.
Only three datasets 1996, 2000, and 2001 include coordinates for camera perspective centers that were captured by onboard GNSS. To aid automated image orientation, they might be utilized as approximations. There are no observations of ground control points (GCPs) available. Except for the ones shot in 1967, which were taken in October, all photograms were taken in the warmer months of June to September.

Year	Acquisition date	Acquisition time	Number of Images	Coordinates of camera	Model of camera	Altitude of flying [km]
2006	Aug 23 - Sep 5	N.A.	78	N.A.	Digital	5.54
2001	Aug 1-13	13 – 15	73	Available	Zeiss RMKTOP15	4.78
2000	Jun 23 - Aug 1	9 – 10	25	Available	Zeiss RMKTOP15	5.54
1996	Jul 3 - Aug 4	7 – 9	35	Available	Zeiss RMKTOP15	5.02
1988	Jul 26	11 – 13	23	N.A.	Leica RC10	6.15
1979	Sep 5	16 – 16:30	19	N.A.	Leica RC10	5.7
1967	Oct 11-12	N.A.	24	N.A.	Leica RC10	6.35

Table 1. Information on photogrammetric data sets over Val Veny that were acquired from the IGNF online repository.

3. PHOTOGRAMMETRIC RECONSTRUCTION

In this section the photogrammetric pipeline for the 3D reconstruction of the surface of Brenva Glacier from multiple data sets is presented. Since historical aerial photos covering the Val Veny span over a 40-years period, the purpose is to monitor the evolution of the glacier from 1967 to 2006.

A number of variables were taken into account while evaluating the image quality. At first, the Val Veny is captured in its entirety in the aerial photos, especially the glaciers. The ground overlap is adequate for aerial triangulation and orthophoto production in flat, hilly, and mountainous terrain. Second, after scanning, the analog photographs were converted into digital data, further degrading the visual quality (Aguilar et al., 2013). Dark shadows may be seen on the photographs as a result of the steep topography that characterizes the mountains surrounding Val Veny. In Figure 3, this issue is shown with an example. Due to the low dynamic range, shadows typically appear as uniform black surfaces (Baumann et al., 2019). Additionally, snow may be an issue since it may smooth down the natural topography of the ground and interfere with image matching algorithms that are used for image orientation and 3D surface reconstruction (Smiraglia et al., 2000).

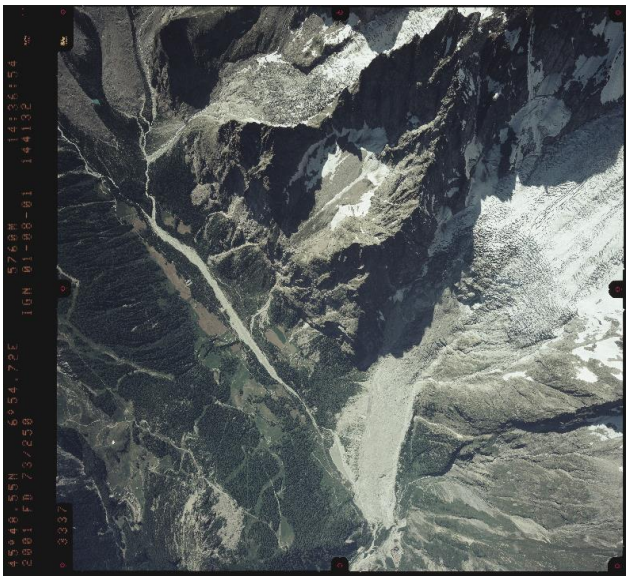

Figure. 3. An illustration of a photo from the 2001 data set with deep shadows on the Brenva Glacier close to vertical surfaces.

The next paragraphs outline the photogrammetric process used to accomplish this goal. The method used here is based on the state-of-the-art method for photogrammetric reconstruction, whereas in the past digital aerial photos were processed using a technique relying on Automatic Aerial Triangulation (Forlani et al., 2000) accompanied by stereo plotting or image matching for DEM generation (Remondino et al., 2014). This features Multi-View Stereo (MVS) dense matching to produce dense point clouds and Structure-from-Motion (SfM) for automated image orientation. This decision was made due to the possibility of employing open-source or standard low-cost photogrammetric software packages, which may be used by many users without degrading the quality of the output point clouds (Barazzetti et al., 2020).
It was decided to use the program Agisoft Metashape® "Professional" ver. 1.7.5. (www.agisoft.com). This well-known standalone program processes digital photographs using photogrammetry and produces 3D spatial data that may be used in various applications.

3.1 Image Pre-processing

Some pre-processing was necessary due to the adopted photographs' poor original quality. The photographs were put into Adobe Photoshop Lightroom Classic 9.4 release® for classification and editing. This application is a professional-grade tool for maintaining photographic collections that is inexpensive, user-friendly, and has effective processing algorithms (Poli et al., 2020). In this study, the radiometric image balancing and correction was employed to reduce variations in the images caused by irregular illumination and the presence of shadows. Clarity and contrast are modified in all data sets in accordance with the unique characteristics of the photographs. This process enhances the functionality of subsequent SfM/MVS matching methods used for dense point cloud creation and image orientation (Haala et al., 2010).

3.2 Structure-from-Motion

The basic objective of SfM is the image orientation, or "Alignment" in software jargon. This stage involves looking for corresponding key-points in photos that may be linked with other images to produce a variety of tie points (Fraser, 2013). This procedure might be sped up and the amount of errors reduced by the availability of approximations for camera stations (for example, from onboard GNSS data). In the absence of these approximations, the image orientation procedure is performed initially to subsampled low-resolution photos before being iteratively transferred to those with full resolution. Agisoft Metashape® was used to run SfM at the maximum quality setting.
A bundle block adjustment (BBA) internal module receives the tie points after which it computes camera calibration parameters, including exterior orientation (EO) parameters, interior orientation (IO) parameters, and the 3D coordinates of tie points. The last ones are utilized to produce the so-called "sparse point cloud" (Eltner et al., 2015), which is subsequently utilized to drive the subsequent MVS dense matching phase (James et al., 2017). The BBA also evaluated camera calibration and EO quality due to numerous photo overlaps, thanks to the data redundancy. Since there haven't been any ground restrictions added yet, the BBA solution was referenced to an arbitrary reference system (e.g., GCPs).

3.3 Georeferencing

Some GCPs were required in order to provide the coordinates of the output 3D point clouds in a geodetic/mapping framework. Sadly, GCPs were not measured in the IGNF historical photographs. Natural features that are consistent over time and across all data sets have been chosen to act as georeference points (GCPs), and their coordinates have been established using the high-resolution satellite data that is currently available. Even though it has been challenging, if not impossible, to search for GCPs in some areas of the area of interest, they have been chosen to be evenly dispersed across each photogrammetric block. In the same line, weak configurations for GCPs have been avoided (Pomerleau et al., 2013). Buildings are typical stable items over time, but they are unfortunately only found in villages and the valley's lower reaches. The task of locating stable areas in glaciers' higher regions has proven to be far more difficult. In all data sets, the same sites (12 in total) were selected as GCPs.
A fresh BBA that includes their observations in the photos has been conducted once a set of GCPs has been chosen. The related ground coordinates have been suitably weighted to prevent distortion in the EO and, as a result, on the output point clouds, due to the poor quality of the observed GCPs.

3.4 Quality Evaluation

The differences between measured coordinates and recently adjusted values are shown by the residuals of the GCPs that BBA provides. Large residual values point to errors in the photogrammetric network of observations. To find the best option, large residuals in GCPs were changed or removed. The nature of these mistakes may result from one of two issues: measurement errors when determining the 3D coordinates of GCPs from satellite observations or measurement errors when determining their 2D coordinates in the photos.
However, deleting too many GCPs might decrease the validity of the photogrammetric model, particularly if several parameters need to be calculated.

3.5 Generation of Dense Point Cloud

The calculated EOs and the "sparse point cloud" were used to generate a dense point cloud after image orientation and camera calibration. Compiling depth maps based on photo discrepancies in normalized image pairings is the initial stage in the MVS process. A dense point cloud is created in a second phase using depth maps (Kaufmann et al., 2003). A combined depth map is constructed by combining the many pairwise depth maps created for each camera, with additional information in overlapping areas being utilized to filter out inaccurate depth readings (Giordano et al., 2017). The depth maps from all of the cameras are merged to create partial dense point clouds, which are then blended together and further noise filtering is done in areas where they overlap to create a final dense point cloud. The dense cloud was then changed to exclude locations that weren't on continuous surfaces, including supraglacial lakes, as well as obvious outliers.
MVS dense matching was done using Agisoft Metashape® with 'high' quality option. Although this option doesn't have the highest theoretical performance, it offers the greatest processing speed and final point cloud quality trade-off.

4. POINT-CLOUD ANALYSIS

4.1 Change Detection

The ice-thickness variation of the Brenva Glacier between 1967 and 2006 was calculated using photogrammetric point clouds derived from historical aerial photographs. No accurate point-to-point correspondences could be used to identify changes because of the nature of point clouds. The comparison could be carried out by using some approaches that may be split in the following groups:

1. By using *algorithms for comparing two point clouds* based on the computation of minimum distances with respect to a given criterion (Tavakoli et al., 2021); and
2. By *interpolating* both point clouds in correspondence of the nodes of the same regular grid (Scaioni et al., 2013). After interpolation, each data set is transformed into raster format and the comparison may be done by differencing the height of corresponding points.

The comparison of point clouds was operated in the open-source software CloudCompare. Ver. 2.11.3 (www. Cloudcompare.org). Before the comparison, each point cloud was pre-processed to improve its quality and to discard

blunders. More details about these tasks can be found in Malekian et al. (2022).
The national geodetic datum (RDN 2008.0 / UTM32N) had been used to georeference all point clouds. Theoretically, this requirement would have been enough to permit direct comparisons across various data sets. Practically speaking, each point cloud's variable quality and the inconsistent precision of the GCP measurements made it harder to match each set of point clouds with one another. Before comparing two point clouds to solve this issue, a co-registration approach was used. To extract the matching point multiple subsets S_i^j and S_i^k, certain stable regions were chosen, and point clouds were segmented. Here, *j* and *k* are the epochs to be analyzed, while *i* is the index indicating the particular subset. After that, the co-registration between the point clouds S_i^j and Sik was improved using subsets S_i^j and S_i^k. To compute the rigid body transformation for reducing the disparities between all relevant subsets S_i^j and S_i^k, the popular ICP (Iterative Closest Points) approach for point cloud alignment implemented in CloudCompare was used. The remaining portions of both point clouds were then finely co-registered by using the transformation parameters (three shifts and three rotation angles) obtained in this manner. In order to demonstrate the precision of the co-registration, the distances between points in stable zones were also measured (Figure 4).

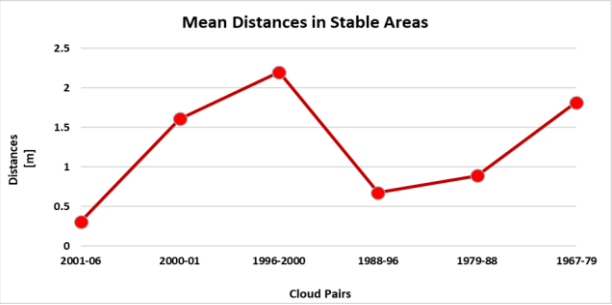

Figure 4. The mean distances in stable parts of the area evaluated in all cloud pairs.

The M3C2 (Multi-scale Model to Model - see Lague et al., 2013) approach was used to identify changes between point cloud pairings following co-registration refinement (see Tavakoli et al., 2021). In the field of geoscience, M3C2 is frequently used to spot variations in three-dimensional point clouds. In reality, the majority of point cloud comparison algorithms in Group (1) and the approaches based on interpolation (Group 2) may show changes in a predetermined direction. On the other hand, M3C2 is based on the reliable computation of local normals, which is utilized to customize the direction to detect changes in each site. Additionally, M3C2 may use information on the precision of the point clouds (if available) to differentiate between true displacements and noise and is resistant to variations in point density and point-cloud noise (James et al., 2017).
Therefore, CloudCompare ver. 2.11.3's M3C2 method was chosen to compare point clouds of the Brenva Glacier.

4.2 Volume Calculations

CloudCompare includes a special function for this objective in order to evaluate the volume change between point clouds of glaciers between two epochs. After choosing a reference plane for use in generating raster DEMs, the volume between the two point clouds is calculated; for further information, see Scaioni et al (2013). The volume is calculated by comparing the DOD (DEM of Differences) between the two DEMs that correspond to the point clouds. The volume is then calculated using the DOD and the area of each raster grid pixel. The accuracy of the estimated volume increases with the size of each elementary cell. On the other hand, the grid step needs to match the point cloud's density (Costa, 1984). More details can be found in Malekian et al. (2022).
Since the most differences between the glacier surfaces computed at different times were along the vertical direction, this technique could be retained adequate for computing volume changes.

5. RESULT AND ANALYSIS

All of the data sets given in Table 1 were processed using the approach described in Section 4. A pre-calibration method was applied before SfM/MVS in the case of data sets photos captured by more than one camera. Following the BBA with GCPs, various quality measurements were taken into consideration to evaluate the outcomes (see Table 2,3). In order to prevent weak configurations, GCPs are selected so that they have at least two projections on the photos and are dispersed as far as is practical over the whole region. Figure 5 reports an instance in point.
Root mean squared errors (RMSEs) on the GCP ground coordinates were between 1 and 4 m, as shown in Table 2. These results, which are also influenced by the changing number and distribution of GCPs, provide information regarding the degree of accuracy of subsequent comparisons (Table 3).
Fiducial marks have been utilized in the BBA for all photogrammetric blocks other than the ones taken in 2006 and 1967. The alignment process can then be carried out either using fiducial marks or by masking them in this situation. The majority of the time, masking the fiducials produced point clouds with better alignment and more density.

Figure 5. The location and distribution of ground control points (GCPs) are shown by an example of a 3D dense cloud reconstruction from the 2001 data set.

Year	RMSE on GCPs ground coord.s		
	XY [m]	Z [m]	Total [m]
2006	1.47	1.38	2.02
2001	3.21	0.33	3.22
2000	2.77	0.68	2.85
1996	3.56	2.45	4.32
1988	4.55	0.69	4.60
1979	3.06	0.20	3.06
1967	0.96	0.94	1.35

Table 2. Root Mean Square Errors (RMSE) of GCPs.

Year	Statistics on tie points		Statistics on GCPs	
	Avg. residuals on image coord.s [pix]	Avg. # tie points per image	Avg. residuals on image coord.s [pix]	Avg. # GCPs per image
2006	0.706	4046	0.621	10
2001	0.714	3835	0.817	10
2000	0.793	3609	0.791	7
1996	0.875	3580	0.799	12
1988	0.896	3830	0.875	6
1979	0.865	3654	0.528	7
1967	0.672	1857	0.309	4

Table 3. statistical parameters after BBA of different photogrammetric blocks.

5.1 Evaluation of Changes in The Brenva Glacier

By using the method described in Subsect. 4.1, 3D point clouds were compared in order to calculate the volume changes of the Brenva Glacier over time. Pairwise comparisons were arranged in accordance with the chronological sequence.
Points inside the i=5 stable windows have been divided and utilized for co-registration refinement depending on ICP to verify the accuracy and dependability of co-registration. The residual distances in these stable windows for each comparison between two epochs, which have been used to estimate co-registration precision, are displayed in Table 4.

Time Period	# Points in sample windows	Mean of M3C2 distances [m]	Std. dev. of M3C2 distances [m]	RMSE of M3C2 distances [m]
2001-2006	436k	0.31	3.80	3.81
2000-2001	396k	1.61	4.39	4.48
1996-2000	177k	1.82	3.82	4.47
1988-1996	150k	0.67	3.10	3.18
1979-1988	233k	0.89	2.38	2.43
1967-1979	243k	1.81	3.58	4.01

Table 4. Residual co-registration errors in five sample windows of stable parts around Brenva Glacier.

The co-registration's precision produced mean differences of between 0.3 and 1.8 meters and RMSEs for distances between 2 and 4.5 meters.
Over a glacier tongue area of around 1.5 km^2, the evaluation of variations in glacier thickness was conducted (Figure 6). The data for the area near the village at the toe of the glacier is lost in the 3D model of Data Set 1979 due to a lack of adequate overlap of photos there. The comparison between point clouds was limited to an extension of approx. 1 km^2 when the 1979 Data Set was adopted. The comparison shows that from 1988 onwards, there has been a significant height decrease of roughly -40 m in certain spots. Until 2000, there was a little gain in ice thickness in the middle, but there was a loss of height in the lower and higher parts. Furthermore, between 2000-2001, there was a major height reduction, indicating a rapid thickness change rate. In comparison to the most recent 3D model (2006), a significant fall in elevation of 15–20 m is apparent at the steep area of Brenva Glacier, while a slight increase of 5–10 m is visible downstream. The Brenva Glacier generally had a minor increment in mass loss until 1996, when there was a dramatic spike in the glacier height changes. A moderate declining tendency is apparent until 2006, but the overall trend for negative glacier mass change rates is growing. Until 1988, the height difference trends revealsmall variations. Then, a highlighted decline is noticeable, which rose to less than -15 meters of height decrease until 1996. This is supported by the growing tendency of the thickness loss rate in Brenva, which has been about -3.5 m/year since 2000. The rate of thickness change for this glacier is then lowered to -1.5 m/year. However it still retains a declining tendency of thickness variation until 2006.

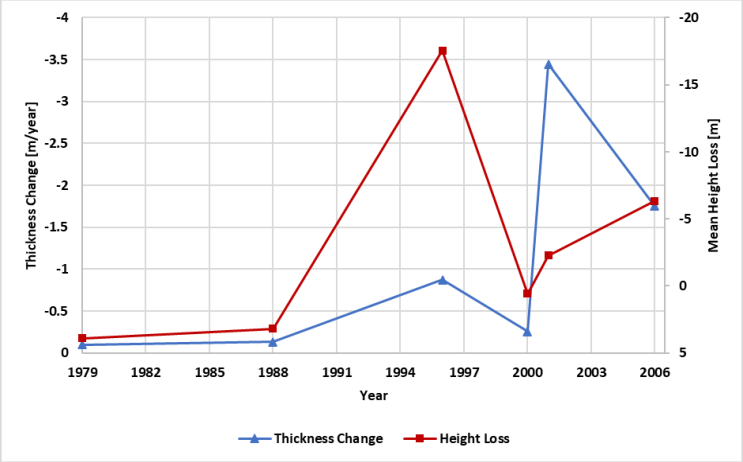

Figure 6. Brenva Glacier's average height and thickness change rate throughout time.

6. DISCUSSION AND CONCLUSIONS

This study used archived images to better comprehend the dynamics and growth of Val Veny's Brenva Glacier from 1967 to 2006. A series of aerial images can be used to analyze morphological changes by using photogrammetric techniques.
The National Geographic and Forestry Institute of France (IGNF) collected this data, which covered an area ranging from 132 km^2 to 345 km^2. During the warmer months of the year, data were collected using a variety of aerial cameras. Comparing the 3D models created from this data allowed researchers to better understand how Brenva Glacier has changed throughout the years.
Following dense Multi-View Stereo matching, the Structure-from-Motion method was used to reconstruct the 3D model of each set of images.
Prior to the primary process, certain pre-processing steps were carried out to enhance key-point extraction from photos. For some data sets, calibration certificates were accessible, making it feasible to test the alignment method using fiducial markers. However, masking the fiducial markers yields better or similar outcomes in the majority of datasets. The initial alignment of the 3D models during the comparison phase was enhanced as a consequence of the usage of satellite data to locate stable points that were utilized as GCPs in all photos. Due to the presence of steep cliffs and bad timing during shooting, the glacier seems to cast shadows in some areas, which causes missing data in some areas of the 3D model.
To analyze differences in Brenva Glacier using 3D models, noise must be removed and model alignment must be precise enough to produce a reliable result. The co-registration quality between two-point clouds may be evaluated using the distances between the stable zones. After co-registration refinement based on ICP, the inaccuracy in the co-registration technique may be assessed in the mean distances in stable regions. Based on the accuracy of the 3D model in each zone of Val Veny, the registration error differs, although it typically ranges between 0.5 and 2 meters. As suggested by other research, particularly for complicated landforms, the multi-scale Model to Model

(M3C2) approach for cloud comparison was used to calculate distances.

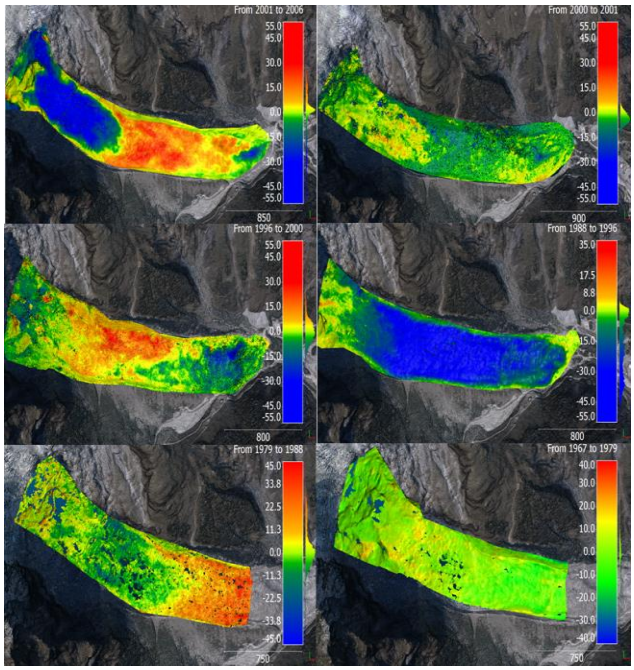

Figure 7. Evolution and distribution of mass loss in Brenva Glacier from 1967 to 2006.

The highest values of height change rate and height reduction among the comparisons are found at Brenva Glacier, which had a height change rate of -3.5 m/year around the beginning of the century. Brenva Glacier is critical in terms of hazard assessment because its closeness to the settlements downstream. Rockfall avalanches in the upper portion and the possibility of a natural dam development downstream as a result of debris flow are the main dangers that might result from the Brenva Glacier.
If archive photos are accessible, the research's technique may be adapted to other applications or places.

Acknowledgements

We would like to acknowledge the National Geographic and Forestry Institute of France (IGNF) for the availability of archive photos. Acknowledgements also go to the developers of CloudCompare open-source software we used in this research,

REFERENCES

Aguilar, M., Aguilar, F., Fernandez, I., Mills, J., 2013: Accuracy assessment of commercial self-calibrating bundle adjustment routines applied to archival aerial photography. *Photogramm. Rec.* 28(141): 96–114.

Barazzetti, L., Gianinetto, M., Scaioni, M., 2020: Automatic Processing of Many Images for 2D/3D Modelling. Digital Transformation of the Design, Construction and Management Processes of the Built Environment, Research for Development, SpringerOpen, Cham (Switzerland), pp. 355-364.

Baumann, P., 2019: *Aerial Photography: History and Georeferencing*. The Geographic Information Science & Technology Body of Knowledge (2nd Quarter Edition), John P. Wilson (Ed.).

Costa, J.E., 1984: Physical geomorphology of debris flows. In: J.E. Costa and P.J. Fleisher (ed.s) *Developments an Applications of Geomorphology*, pp. 268–317, Springer-Verlag, Berlin.

Eltner, A., Kaiser, A., Castillo, C., Rock, G., Neugirg, F., Abellán, A., 2015: Image-based surface reconstruction in geomorphometry – merits, limits and developments. *Earth Surf. Dyn.*, 4: 359-389.

Fey, C., Wichmann, V., Zangerl, C., 2017: Reconstructing the evolution of a deap seat-ed rockslide (Marzell) and its responseto glacial retreat based on historic and remote sensing data. *Geomorph.*, 298: 72-85.

Forlani G., Pinto L., Scaioni M., 2000: Concept and Testing of an Automatic System for Aerial Triangulation. *Int. Arch. Photogramm. Remote Sens.*, Vol. 33, Part B2: 486-493.

Fox, A.J. and Cziferszky, A., 2008: Unlocking the time capsule of historic aerial photography to measure changes in Antarctic peninsula glaciers. *Photogramm. Rec.*, 23(121): 51–68.

Fraser, C.S., 2013: Automatic camera calibration in close range photogrammetry. *Photogramm. Eng. Remote Sens.*, 79(4): 381-388.

Fugazza, D., Scaioni, M., Corti, M., D'Agata, C., Azzoni, R.S., Cernuschi, M., Smiraglia, C., Diolaiuti, G.A., 2018: Combination of UAV and terrestrial photogrammetry to assess rapid glacier evolution and map glacier hazards. *Nat. Hazards Earth Syst. Sci.*, 18: 1055–1071.

Fugazza, D., Senese, A., Azzoni, R.S., Smiraglia, C., Cernuschi, C., Severi, D., Diolaiuti, G.A., 2015: High-resolution mapping of glacier surface features. The UAV survey of the Forni Glacier (Stelvio National Park, Italy). *Geografia Fisica e Dinamica del Quaternario*, 38: 25-33.

Giordano, S., Le Bris, A., Mallet, C., 2017: Fully automatic analysis of archival aerial images current status and challenges. In: Proc. 'Joint Urban Remote Sensing Event (JURSE)'.

Haala, N. Kada, M., 2010: An update on automatic 3D building reconstruction. *ISPRS J. Photogramm. Remote Sens.*, 65: 570-580.

James, M.R., Robson, S., Smith, M.W., 2017: 3-D uncertainty-based topographic change detection with structure-from-motion photogrammetry: precision maps for ground control and directly georeferenced surveys. *Earth Surf. Proc. Landforms*, 42(12): 1769-1788.

Kaufmann, V., Ladstädter, R., 2003: Quantitative Analysis of Rock Glacier Creep by Means of Digital Photogrammetry Using Multi-Temporal Aerial Photographs: Two Case Studies in the Austrian Alps. In: Proc. '8th Int. Conf. on Permafrost,' Zurich, 21–25 July 2003, pp. 21–25.

Koblet, T., Gärtner-Roer, I., Zemp, M., Jansson, P., Thee, P., Haeberli, W., and Holmlund, P., 2010: Reanalysis of multi-temporal aerial images of Storglaciären, Sweden (1959–99) – Part 1: Determination of length, area, and volume changes, The Cryosphere, 4, 333–343.

Kraus, K., 2008: *Photogrammetry - Geometry from Images and Laser Scans*. Walter de Gruyter, Berlin.

Lague, D., Brodu, N., Leroux, J., 2013: Accurate 3D comparison of complex topography with terrestrial laser scanner: Application to the Rangitikei canyon (N-Z). *ISPRS J. Photogramm. Remote Sens.*, 82: 10-26.

Malekian, A., Fugazza, D., Scaioni, M., 2022: 3D Surface Reconstruction and Change Detection of Miage Glacier (Italy)

from Multi-date Archive Aerial Photos. In: O. Gervasi et al. (Ed.s.), *ICCSA 2022 Workshops*, LNCS 13379, pp. 450–465.

Poli, D., Casarotto, C., Strudl, M., Bollmann, E., Moe, K., Legat, K., 2020: Use of Historical Aerial Images for 3D Modelling of Glaciers in the Province of Trento. *ISPRS Int. Arch. Photogramm. Remote Sens. Spat. Inf. Sci.*, Vol. 43, Part B2: 1151–1158.

Pomerleau, F., Colas, F., Siegwart, R., Magnenat, S., 2013: Comparing ICP variants on real-world data sets. *Autonomous Robots*, 34: 133–148.

Remondino, F., Spera, M.G., Nocerino, E., Menna, F., Nex, F., 2014: State of the art in high density image matching. *Photogramm. Rec.*, 29: 144–166.

Scaioni, M., Roncella, R., Alba, M.I., 2013: Change Detection and Deformation Analysis in Point Clouds: Application to Rock Face Monitoring. *Photogramm. Eng. Remote Sens.*, 79(5): 441-456.

Scaioni, M., Barazzetti, L., Yordanov, V., Azzoni, R.S., Fugazza, D., Cernuschi, M., Diolaiuti, G.A., 2019: Structure-From-Motion Photogrammetry to Support the Assessment of Collapse Risk in Alpine Glaciers. In: O. Altan et al. (Ed.'s), Intelligent Systems for Crisis Management. Gi4DM 2018, LNGC, Springer, Cham (Switzerland), pp. 239-263.

Scaioni, M., Corti, M., Diolaiuti, G., Fugazza, D., Cernuschi, M., 2017: Local and general monitoring of Forni glacier (Italian alps) using multi-platform structure-from-motion photogrammetry. *Int. Arch. Photogramm. Remote Sens. Spatial Inf. Sci.*, Vol. 42, Part 2/W7: 1547-1554.

Scaioni, M., Crippa, J., Corti, M., Barazzetti, L., Fugazza, D., Azzoni, R., Cernuschi, M., Diolaiuti, G.A., 2018: Technical Aspects Related to the Application of SfM Photogrammetry in High Mountain. *Int. Arch. Photogramm. Remote Sens. Spatial Inf. Sci.*, Vol. 42, Part 2: 1029-1036.

Smiraglia, C., Diolaiuti, G., Casati, D., Kirkbride, M., 2000: Recent areal and altimetric variations of Miage Glacier (Monte Bianco Massif, Italian Alps). In: Nakawo, M., Raymond, C.F., and Fountain, A. (eds), Debris-Covered Glaciers IAHS Publ. 264, pp. 227–233.

Tavakoli, K., Zadehali, E., Malekian, A., Darsi., Longoni, L., Scaioni, M., 2021: Landslide Dam Failure Analysis Using Imaging and Ranging Sensors. In: Proc. 'ICCSA 2021', LNCS 12955, pp. 3–17.

Wikipedia, Marmolada serac collapse. Available online at https://en.wikipedia.org/wiki/ 2022: Marmolada_serac_collapse (last access on 22nd September2022.